RSC Advances

PAPER

View Article Online
View Journal | View Issue

Cite this: *RSC Adv.*, 2015, **5**, 57875

Control of co-existing phases and charge transport in a nanostructured manganite film by field effects with an electric double layer as the gate dielectric

Rajib Nath* and A. K. Raychaudhuri

Received 15th May 2015
Accepted 15th June 2015

DOI: 10.1039/c5ra09081d

www.rsc.org/advances

We report bipolar control of co-existing phases in a nanostructured film of manganite, $La_{0.85}Ca_{0.15}MnO_3$, using an applied gate bias in a field effect (FE) device configuration. Low hole-doped manganite $La_{0.85}Ca_{0.15}MnO_3$ shows the co-existence of different electronic phases and a ferromagnetic insulating (FMI) state at low temperatures. The FE device with manganite as the channel uses an electric double layer (EDL) as a gate dielectric which can induce a large specific charge density ($\geq 10^{13}$ cm^{-2}) in the channel when a moderate gate bias is applied. The nanostructured nature of the manganite film enhances the field effect by controlling transport within the nano-grain as well as by controlling the depletion layer and the potential barrier at the grain boundaries. We observed a large modulation in the resistance of the film, $\sim\pm 40\%$, at room temperature for a moderate gate bias (V_G) of ± 4 V, which increased to $\sim\pm 100\%$ at 100 K. The field-effect-induced charges alter the relative fraction of the co-existing phases as well as the characteristic temperatures, such as the orthorhombic–orthorhombic (O–O′) transition temperature, the ferromagnetic transition temperature, and the onset temperature of the low temperature FMI state. The change in the relative fraction of the phases was found to have an exponential dependence on the gate bias. By using the shift in the temperature of the O–O′ transition with gate bias as a reference, we could establish that the change in hole concentration, brought about by the field effect, closely mimics (quantitatively) the changes brought about *via* chemical substitution, including the change in the activation energy of transport in the paramagnetic insulating region.

1 Introduction

The control of electronic phases and electrical transport in a strongly correlated oxide film through a field effect (FE), using a gate with an electric double layer (EDL), is a topic of considerable current interest.[1–4] The electrolyte is used as a gate dielectric and forms an EDL at the solid–electrolyte interface, which in turn leads to a large specific gate capacitance that can induce a substantial surface charge density ($\geq 10^{13}$ cm^{-2}) for a moderate applied gate bias.[5–7] This induced surface charge density is orders of magnitude larger than that induced by conventional oxide gate insulators such as SiO_2 or $SrTiO_3$ for the same bias. Thus, the large induced surface charge density can control the electrical transport in strongly correlated oxides (such as transition metal perovskites), which depends on the carrier density and often on co-existing electronic phases with differing electrical resistivities, as in hole-doped manganites. The native carrier density is very high in the case of transition metal oxides. The induced charge/carrier density from FEs with a gate dielectric should be large in order to produce any observable modulation in these oxides. The large modulation in the carrier density can be achieved using an EDL dielectric. Modulation of the carrier density by the FE with a gate dielectric containing an electrolyte or ionic liquid gives rise to various interesting phenomena, such as metal–insulator transitions,[8,9] superconductivity[1,10] or the control of the conduction at the grain boundary (GB) region in a functional perovskite.[11] The advantage of the FE-induced carrier modulation is that it overcomes the collateral problem of disorder that accompanies carrier modulation *via* chemical substitution.

In this paper, we show that the nanoscopic control of co-existing phases (and through it, control of the electronic transport) can be obtained in nanostructured films of functional oxides, such as hole-doped manganites, using an EDL-FET device structure. The control can be bipolar in nature with a positive (negative) gate bias depleting (enhancing) the hole density. We show that the change in the hole density closely mimics the changes that can be brought about using chemical substitution, including structure-related transitions such as the orthorhombic–orthorhombic (O–O′) transition seen in manganites. In this report, we determine the role of the gate-bias controlled transport through the grain boundary (GB) region in nanostructured manganite films. The role of the GB in controlling charge transport in manganites is well established,

Dept. of Condensed Matter Physics & Material Sciences, S. N. Bose National Centre for Basic Sciences, Salt-lake, Kolkata-98, India. E-mail: rajibnath.bu@gmail.com; arup@bose.res.in

particularly in the context of its contribution to magnetoresistance.[12] In nanostructured manganites, GB transport takes place across the GB potential barrier *via* tunneling.[13–16] However, the control of the GB barriers by the field effect through an applied gate bias has not been adequately addressed in nanostructured manganites. In this paper, we address this issue. We show that the control of GB transport by an applied gate bias occurs in tandem with control of transport within the grain by the FE. This in turn leads to substantial control over the co-existing phases. The control of the GB transport by the FE, though done in the specific context of manganites, can be expected to have a more general application in GB-controlled transport in many nanostructured oxide films.

The work was carried out in a nanostructured film of low-hole-doped manganite ($La_{1-x}Ca_xMnO_3$) with $x \sim 0.15$ grown on a SiO_2/Si substrate. We have chosen the SiO_2/Si substrate to make the film nanostructured. In a nanostructured film, the FE-induced charge can bring about effective control of transport at two distinct levels. First, it occurs within a grain of the oxide (intra-grain), and second, it can control the potential barrier that forms in the GB region, and thus can control the inter-grain charge transport. In a recent paper,[11] we have shown that a gate with an EDL dielectric can control the depletion layer in the GB regions.

The choice of the low hole-doped manganite $La_{1-x}Ca_xMnO_3$ (LCMO) is mainly motivated by the fact that it has co-existing electronic phases that vary with temperature. This gives rise to an interesting system where the proposed effects can be observed and investigated. In hole-doped manganites such as LCMO, one can obtain different phases as a function of chemical substitution x, which in turn controls the hole concentration. LCMO evolves from an orbitally ordered antiferromagnetic insulating (AFMI) phase ($x = 0$) to a ferromagnetic (FM) metallic phase that occurs for $x \geq 0.22$.[17–19] In the intermediate region with $x \sim 0.15$, the material shows a ferromagnetic insulating (FMI) phase at low temperatures. In this composition range, it shows the coexistence of different phases with different conductivities and different magnetic orders that can occur below its ferromagnetic ordering temperature. We have shown that the application of a gate bias that induces a large carrier density can control the relative fraction of the coexisting electronic phases, leading to a large change in the transport properties. In a nanostructured film, this effect is enhanced due to the formation of an effective "all-around-gate" by the polymer electrolyte as it flows in the GB region during its solidification. The change in the resistance of the film can be large, and one can obtain bipolar control as the gate bias (V_G) is changed from negative to positive. The film resistance is changed by nearly $\pm 40\%$ at room temperature with a moderate change in the gate bias V_G of ± 4 V, where the negative bias reduces the resistance. At lower temperatures, the effect is significantly enhanced whereby a change of similar magnitude in the gate bias can change the channel resistance by one order. The applied bias not only changes the resistance, but also affects the temperature range over which the co-existing phases are observed and also changes the activation energy for transport in the polaronic paramagnetic insulating state that occurs above the ferromagnetic temperature. This mimics the change in the hole concentration brought about *via* chemical substitution, which we could quantitatively monitor by tracking the change in the O–O′ transition as a function of the applied gate bias V_G.

2 Experimental

The experiment was conducted in a field effect transistor (FET) device configuration using an EDL as the gate dielectric. The device was fabricated with a thin film channel (with an effective length of 1 mm and width of 300 μm) of $La_{0.85}Ca_{0.15}MnO_3$ on a SiO_2 (300 nm)/Si substrate using a stoichiometric target. A thin film channel of thickness $\approx$ 10 nm was grown by pulsed laser deposition using an excimer laser with a fluence of 1 J cm^{-2} in 0.1 mbar O_2 pressure.[11] An atomic force microscopy image of the film (shown in Fig. 1(b)) shows an island type growth pattern with bimodal distribution of grains, sized 3 & 22 nm.[11] The source (s) and drain (d) contact pads were made using thermally evaporated Au/Ti. The source and drain pads were protected from the polymer electrolyte by a layer of an e-beam resist (PMMA), baked for 3 min at 180 °C. The dielectric was applied through a window (opening) in the resist layer on the channel. We used a PEO : $LiClO_4$ (10 : 1) electrolyte mixture as the gate dielectric.[11] A Cu wire was used as the gate contact. A schematic of the device and the corresponding electronic circuit is shown in Fig. 1(a). We performed the *I–V* measurement of the channel with $V_G = 0$ V.[11] The *I–V* curve is symmetric due to the identical s and d electrodes having negligible contact resistance. The temperature dependent measurements were carried out in a closed-cycle variable temperature cryostat with a cryo-cooler. The channel resistance R was measured in a constant current mode (the drain current I_{DS} was fixed), and the source–drain voltage (V_{DS}) was measured with a source meter using the FET configuration shown in Fig. 1(a). The *R–T* curves of the channel at different V_G were measured using a current of 1 μA. Another source-meter was used to apply the gate bias V_G and to detect the gate current I_G as shown in Fig. 1(a). The gate current (I_G) in the steady state is much less than the channel current, I_{DS}, which ensures low leakage at the gate. We also measured the

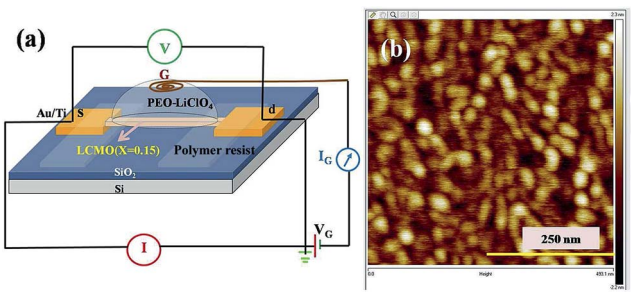

Fig. 1 (a) Schematic diagram of the EDL-FET device with the LCMO channel, where s, d & G represent the source, drain and gate electrodes. The contact pads at the s and d regions are protected from the gate electrolyte by a resist layer composed of an insulating polymer. (b) The AFM topograph of the nanostructured LCMO channel in an area $\approx$ 500 nm $\times$ 500 nm.

transient gate current $I_G(t)$ in response to a step change in the gate bias V_G in order to determine the capacitance of the gate, which we used to measure the amount of induced charge for a given gate bias.

3 Modulation of the channel resistance and the characteristic temperatures by the field effect

The device made with the LCMO $x = 0.15$ channel shows a symmetric *I–V* curve and the *I–V* curve is linear for a low applied bias ($V_{DS} \leq 0.5$ V).[11] To ensure that the resistance measurements were carried out within the linear ohmic region, we have measured the resistance of the channel using a low constant current so that the voltage across the source–drain (V_{DS}) is less than 0.5 V. The *R vs. T* curves with different gate biases (V_G) varying from +4 V to −6 V are shown in Fig. 2. The relative change in the resistance of the channel at room temperature due to the change in the applied V_G is nearly ±40%. The change in *R* is enhanced at low temperatures. For instance, at $T = 100$ K, the channel resistance *R* changes from nearly 3 Mohm to 0.2 Mohm with decreasing V_G from +4 V to −6 V. The evolution of the channel resistance as a function of gate bias V_G is also accompanied by a shift in some of the characteristic temperatures, indicating a transformation between the different co-existing phases in the film. This can be appreciated from the changes in the shapes of the *R–T* curves with different V_G. To identify these temperatures clearly, we have taken the derivatives of the *R–T* curves, as shown in Fig. 3. In the figure, we plot $\frac{d(\ln RT^{-1})}{dT^{-1}}$ as a function of *T* at $V_G = 0$ V and at two representative V_G values. The derivative curve accentuates the three characteristic temperatures clearly as a deviation from a smooth temperature variation. These temperatures are marked in Fig. 3. However, the identity of these characteristic temperatures cannot be inferred from the *R–T* curve alone as doing so requires the use of a multitude of other techniques that are difficult to perform directly on a thin film in the FET configuration. Therefore, we have used a known phase diagram of LCMO (as a function of *x*),[17–19] to identify these temperatures from the derivative curve at $V_G = 0$ V.

From the evolution of the derivative curves, we tracked how these temperatures change with V_G. The co-existence of different phases in low-doped manganites like LCMO $x = 0.15$ is known from past investigations.[17–19] This phase coexistence can be perturbed by temperature or by external stimuli like pressure; in our case it is the charge induction of the channel using the electrolytic gate. The gating actually controls the intra-grain transport (by modulating the carriers) as wells as the inter-grain conduction by modulating the GB potential barrier[11] of the channel. In LCMO $x = 0.15$, there are 3 regions (regions I, II, and III) that can be identified. Region I is a low-temperature

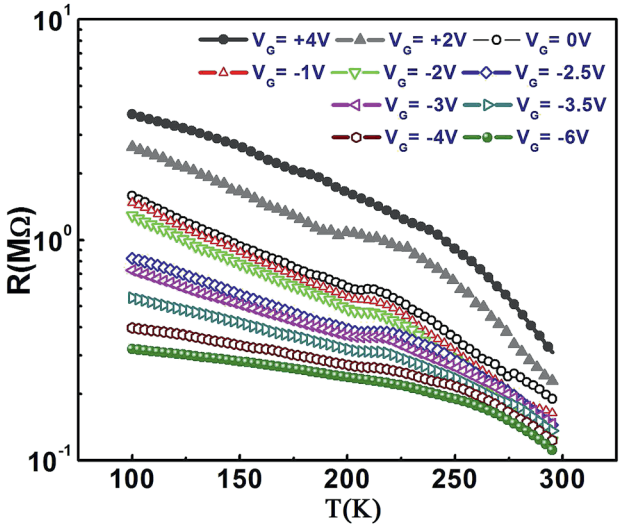

Fig. 2 *R–T* curves of the channel with different gate biases. A positive gate bias enhances *R* while a negative bias suppresses *R*.

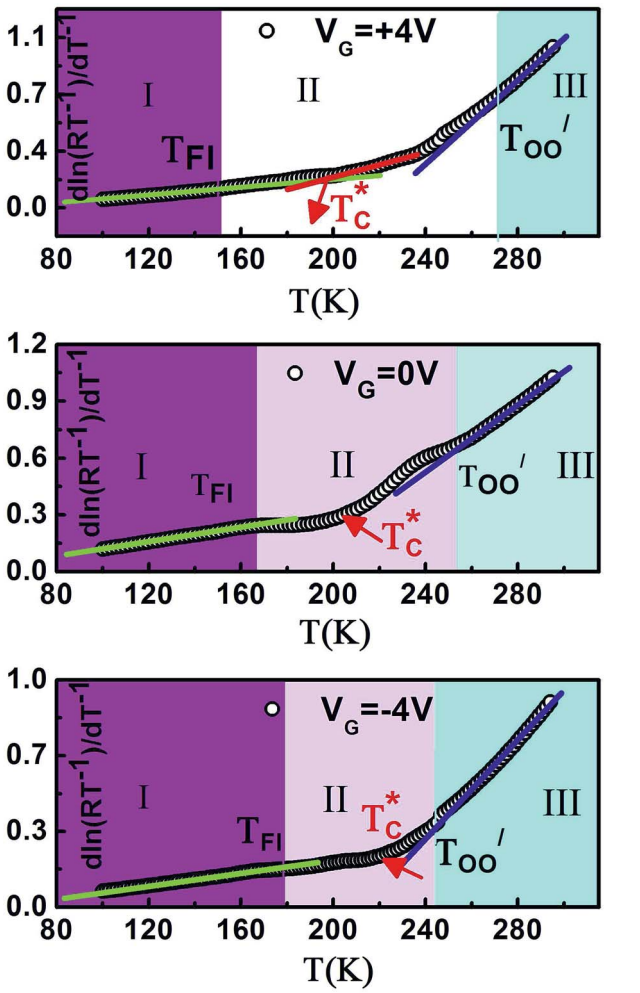

Fig. 3 The characteristic temperatures of the LCMO channel are marked as determined from the transport data by plotting normalized $\frac{d(\ln RT^{-1})}{dT^{-1}}$ *vs. T* at $V_G = +4$ V, 0 V and −4 V, respectively. The color boundaries indicate the different characteristic regions with their temperatures T_{FI} (color boundary for region I) and $T_{OO'}$ (color boundary for region III). The red arrow represents the position of T_C^*.

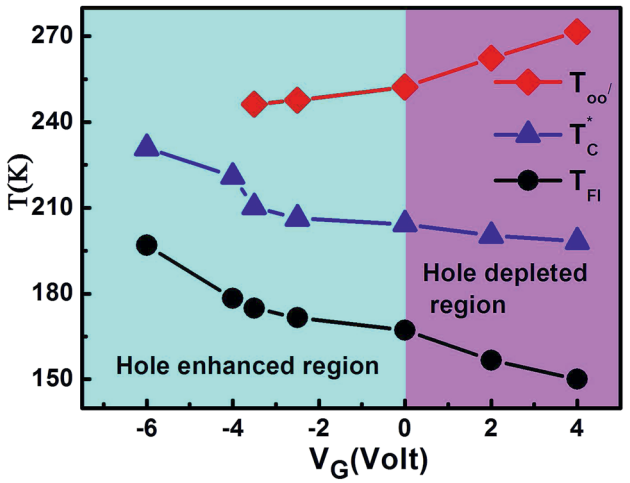

Fig. 4 Variation of the characteristic temperatures $T_{OO'}$, T_C^* and T_{FI} as a function of gate bias. The characteristic temperatures are obtained from Fig. 3.

ferromagnetic insulating state (FMI), the onset of which is marked by the temperature T_{FI}, which in turn also changes with hole concentration. Region II is a predominantly mixed phase region with a co-existing low resistance FM phase (which may be a high resistive metallic phase having a shallow T dependence and a high-resistance insulating phase). There is also a paramagnetic to ferromagnetic transition that shows up as a change in the slope of the R–T curve. This we mark as the temperature T_C^* (note: we distinguish this from the ferromagnetic transition temperature T_C, which is determined from magnetic measurements. The temperatures T_C^* and T_C may be close but not necessarily the same. However, for our film, for $V_G = 0$, the T_C^* determined from the derivative curve matches with the T_C value, as determined using magnetic measurements). In region III, the system is in a paramagnetic insulating (PI) state with an orthorhombic phase (O phase). It undergoes structural distortion due to the onset of a cooperative Jahn–Teller (JT) transition and assumes a distorted orthorhombic structure with rotated octahedra marked as the O′ phase (note: resistivity data taken on single crystals also show this transition as a change in the slope when the O–O′ transition is determined crystallographically[20,21]). The transition temperature, marked as $T_{OO'}$ in Fig. 3, is an important marker for the hole concentration as it is decreased at increasing hole concentrations.[21] The characteristic temperatures obtained from the $\frac{d(\ln RT^{-1})}{d(T^{-1})}$ *vs.* T curve at $V_G = 0$, as shown in Fig. 3, match well with the reported data for LCMO $x = 0.15$.[17–19] The application of a V_G of either polarity shifts these temperatures. In Fig. 4, we show the evolution of the three temperatures ($T_{OO'}$, T_C^* and T_{FI}) as a function of the gate bias. All three temperatures show substantial change upon application of a moderate gate bias. Importantly, the change is bipolar with a positive (negative) V_G that leads to hole depletion (enhancement), thereby depressing (raising) T_C^* and raising (depressing) $T_{OO'}$. We show below that the changes brought about by the gate-induced charges (FE-induced charges) mimic the changes that one would expect with a change in the hole concentration (δx) in $La_{1-x}Ca_xMnO_3$ brought about *via* chemical substitution.[17–19] The variation in the characteristic temperatures with the gate bias is closely related to the change in the relative fraction of the co-existing phases that we will discuss in later sections. The observation that one can tune the temperature T_{FI}, as well as $T_{OO'}$, using an applied gate bias is new and is a direct manifestation of the fact that the FE-induced charges can change the hole concentration in a manner similar to that achieved *via* chemical substitution.

4 The field effect and induced charge in the channel

The observed bipolar modulation of the channel resistance arises from the modulation of the carrier density due to the application of a finite gate bias. The electric field due to the formation of an EDL near the electrolyte–channel interface affects the carrier concentration in the channel, mostly over a length scale in the order of the Debye length from the surface.[22,23] We have calculated the Debye length (λ_D) of the sample using the equation $\lambda_D = \sqrt{\frac{\varepsilon_r \varepsilon_0 \kappa_B T}{n_{3D} e^2}}$, where ε_0 is the permittivity of free space, ε_r is the dielectric constant of the material, κ_B is the Boltzmann constant, e is the electronic charge and n_{3D} is the volume carrier density in the channel. We obtained $\lambda_D \approx 4$ nm at $T = 300$ K using the value of ε_0, $n_{3D} \approx 10^{21}$ cm^{-3} and $\varepsilon_r \approx 100$ (for LCMO).[24] The estimated λ_D is comparable to the average grain size ($\approx$3 nm) of the film, and the film thickness, though somewhat large, is also comparable ($\approx 2.5\lambda_D$) to this length scale. Since the electrolyte flows around the grains during its solidification, we may assume that the entire thickness of the channel is affected more or less uniformly by the field-induced charge, and an effective carrier density modulation can be achieved by the applied gate bias V_G. In Fig. 5, we show schematically the effect of the gate bias on the channel–electrolyte interface, which modulates the carrier density as well as the GB potential barrier.

5 A quantitative comparison of the change in the hole concentration achieved by the gate induced FE and that achieved *via* chemical doping (δx)

In the previous section, we observed that a moderate gate bias can be used to tune R, its temperature dependence, and it can also substantially affect the characteristic temperatures ($T_{OO'}$, T_C^* and T_{FI}). In this section, we will quantitatively compare the changes brought about by the gate-induced carriers with those expected from chemical doping (δx). We estimate the change in hole concentration (δx) from the shift in $T_{OO'}$, as achieved by the field effect, and compare it with the change in hole concentration calculated from the gate bias and the specific gate capacitance that gives the electrostatically induced charge density. An enhanced hole concentration lowers the $T_{OO'}$.[17–19,21] Since the change in $T_{OO'}$ as a function of x (brought about *via* chemical

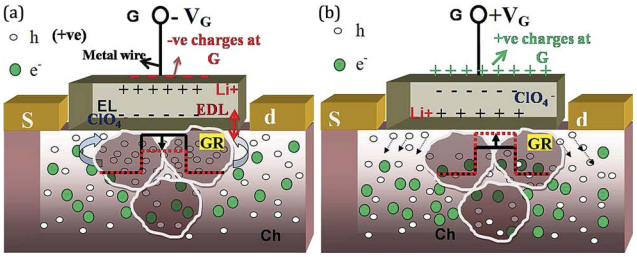

Fig. 5 Schematic diagram of the effect of (a) $-V_G$ and (b) $+V_G$ within the channel. s, d & G are the source, drain & gate electrodes; EL & Ch represent the electrolyte and the channel; h, e^-, and GR represent the holes, electrons and grains. The black rectangular well represents the GB potential barrier at $V_G = 0$ V. The red (dashed) rectangular well represents the barrier potential at GB at $-V_G$ or $+V_G$.

substitution) is well established, its change with gate bias can thus be used as a calibrated measure of the effective change in hole concentration δx due to the change in V_G.

In our previously reported experiment, we measured the transient gate current $I_G(t)$ in response to a step change in the gate bias V_G.[11] The analysis of the transient gate current has been used to obtain the gate capacitance (C_g) from the charging time constant (R_gC_g), where R_g is the gate resistance through which the gate capacitance charges. From the measured C_g, we obtain a specific gate capacitance ≈ 1.6 μF cm^{-2}. We estimate an induced surface charge density of 1×10^{13} cm^{-2} for a gate bias of 1 V. Using the value $\lambda_D \approx 4$ nm at $T = 300$ K and the assumption that induced carriers can affect the carrier density in the channel over a depth roughly equal to the Debye length from the surface, $\sim\lambda_D$, we find a volume charge density of $\sim 0.5 \times 10^{19}$ cm^{-3} for a gate bias change of 1 V. From the formula unit volume of ~ 60 Å^3 for LCMO, we find that the induced carrier density causes a change of $\delta x \approx \pm 0.0013$/formula unit for $V_G = \pm 1$ V. To distinguish this δx, obtained from the electrostatic method, from that obtained *via* chemical substitution, we call it δx_e to mean that this has been brought about by an electrostatic effect. In Fig. 6, we show δx_e as a function of V_G. This shows the change in hole concentration expected from a gate-induced field effect.

We have calculated the modulation of δx with the variation of $T_{OO'}$ from the known linear variation of $T_{OO'}$ with x in $La_{1-x}Ca_xMnO_3$ when x is changed *via* chemical substitution, as documented in the phase diagram of $La_{1-x}Ca_xMnO_3$.[17–19] From the data, we find that a lowering of 1 K in $T_{OO'}$ occurs due to an enhancement in δx of $\sim 3 \times 10^{-4}$. From Fig. 4, we could thus calculate the variation of δx as a function of $\pm V_G$. In Fig. 6, we show the variation of δx with V_G along with δx_e. From Fig. 6, it can be seen that the estimated values of δx from $T_{OO'}$ and δx_e derived from the FE-induced charge are nearly the same in the positive gate voltage region ($+V_G$). It is of a similar order, but is somewhat different in magnitude in the negative gate voltage ($-V_G$) region. It is indeed gratifying that δx and δx_e, though estimated from two independent methods, give similar values. It establishes that the change in hole concentration as a result of the field effect (using the EDL dielectric) is predominantly an electrostatic effect. There is a difference between δx & δx_e in the negative gate bias region where we find that $\delta x < \delta x_e$. This implies that hole accumulation within a grain due to the field effect is less than that expected from a simple electrostatic effect. This difference likely arises from the fact that parts of the induced holes (being majority carriers) compensate the heavily depleted GB region. In such nanostructured films, the GB region being strongly depleted of majority carriers, forms a depletion region.[11] A part of the FE-induced charge leads to the lowering of the GB potential barrier and narrowing of the depletion layer (shown schematically in Fig. 5). For a positive gate bias, where the hole concentration is reduced with gate bias, the GB region is depleted further (shown schematically in Fig. 5). This makes the value of δx closer to that of δx_e but $|\delta x|$ is somewhat larger than $|\delta x_e|$.

6 Dependence of the activation energy of transport on the gate bias

In the temperature range $T > T_C^*$, the charge transport is strongly activated with an activation energy E_a. The charge transport within a grain is polaronic in nature and it has a polaronic origin. In manganites, E_a can be affected by structural changes (due to external pressure), the presence of the GB potential barrier or defects present in the system.[25–27] Here, we observed that the FE-induced charges and the modulation of the GB potential barrier play an important role in changing the E_a of the channel. The change in E_a with the gate bias V_G can be compared qualitatively to the change in E_a, that can arise from hole doping by substitution (a change in x).[20] The applied gate bias can lead to the modulation of both the polaronic contribution to E_a and the contribution arising from the GB barrier. In the temperature region of interest ($T > T_C^*$ at $V_G = 0$ and at negative V_G), owing to the lowering of the GB barrier by the induced hole, it is expected that the activation energy E_a will predominantly be of polaronic origin following the equation $R = R_0 T \exp\left(\frac{E_a}{\kappa_B T}\right)$.[20] It has been known from past studies on

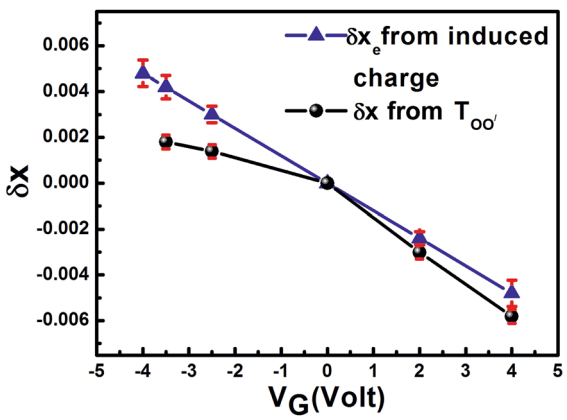

Fig. 6 Variation of δx and δx_e with different values of V_G, calculated from the induced charge due to the field effect (δx_e) and from the change in $T_{OO'}$ (δx).

single crystals[20] that the activation energy E_a is suppressed by the enhancement of x (the enhancement of the hole doping). Thus the reduction in E_a with an applied negative gate bias can be understood. For a positive gate bias, where the hole density is depleted, one would expect E_a to increase. However, the magnitude of the change of E_a in this region is very steep and is more than what one would expect from a change in hole density alone (Fig. 7).[20] It is likely that the steep change in E_a is a reflection of the enhancement of the GB barrier that can occur due to a strongly depleted GB region.

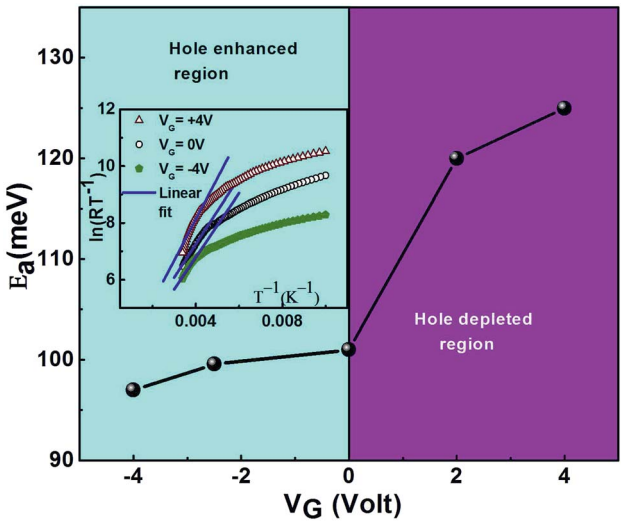

Fig. 7 Variation of E_a with different values of V_G. The inset shows the adiabatic polaronic fits to the R–T data at V_G = +4 V, 0 V & −4 V, respectively, from which E_a are determined at different V_G.

7 Control of coexisting electronic phases by the gate bias

The evolution of channel resistance R as a function of temperature T as well as gate bias V_G can be phenomenologically explained as arising from the evolution of the relative fraction (f) of the two co-existing phases in the channel. The transport in regions I and II takes place predominantly through the two co-existing phases: one, a high-resistance insulating phase (resistance denoted by R_{ins}), and the other, a low-resistance 'marginally' metallic phase, whose resistance is denoted by R_m (we call it metallic for reference purposes only). It can be a high resistive metallic phase (having higher resistance than the normal metals) with relatively lower resistance than the insulating phase. Changes in T and V_G alter the relative fraction f of the two co-existing phases. Thus the change in f can phenomenologically describe the change in R as a function of T and V_G. The transport and magnetic properties in low-hole-doped manganites ($x \leq 0.2$) have been explained using such co-existing phases as stated before.[19]

A change in the intra-grain hole concentration will alter the relative fraction of the coexisting phases; however, the observed effective f will also depend on the conductivity of the GB region. For a negative gate bias that reduces the GB potential barrier due to an increase in the number of holes, one would see an enhancement of the effective f over and above that expected from changes within a grain alone. Similarly, a gate-bias-induced enhancement of a GB potential that occurs at positive V_G will contribute to a reduction of the effective f. Thus, in the nanostructured film, the potential barrier at the GB will affect the effective f.

We obtain an estimate of f from a simple 2-phase model for conduction. In the presence of two such phases, the channel resistance (R) can be expressed as

$$\frac{1}{R} = \frac{(1-f)}{R_{ins}} + \frac{f}{R_m}, \quad 0 \leq f \leq 1, \tag{1}$$

We have assumed $R_{ins}(T)$ to be the resistance of the channel at V_G = +4 V. The rationale for this assumption is that the hole depletion at positive bias converts the channel into a high-resistance insulating phase with a metallic fraction ($f \rightarrow 0$) along with the highly depleted GB region with an enhanced GB barrier. $R_m(T)$ is taken as the resistance of the channel at V_G = −6 V, where we assume that the entire channel, by the enhancement of hole concentration, has only the 'metallic' phase ($f \rightarrow 1$) with a reduction in the depletion region and the GB barrier potential. From eqn (1), we obtained f as a function of T for different gate bias (V_G) values. We have limited our analysis to $T < T_{OO'}$ where we have the mixed-phase region. In Fig. 8, we have plotted the metallic fraction (f) *vs.* T curves at different V_G. Fraction f can be written as $f(T,V_G)$ since it is a function of both T and V_G as seen in Fig. 8. At $T \leq 240$ K, for all gate bias values, $f(T,V_G)$ decreases on cooling due to the activated nature of the transport in the channel as well as due to the barrier in the GB region. However, the temperature dependence becomes less steep as V_G becomes more negative and f increases. The temperature dependence is more steep when V_G > 0, which depletes the hole density in the channel, thus enhancing the insulating fraction of the coexisting phases. A negative V_G, which leads to the accumulation of more holes in

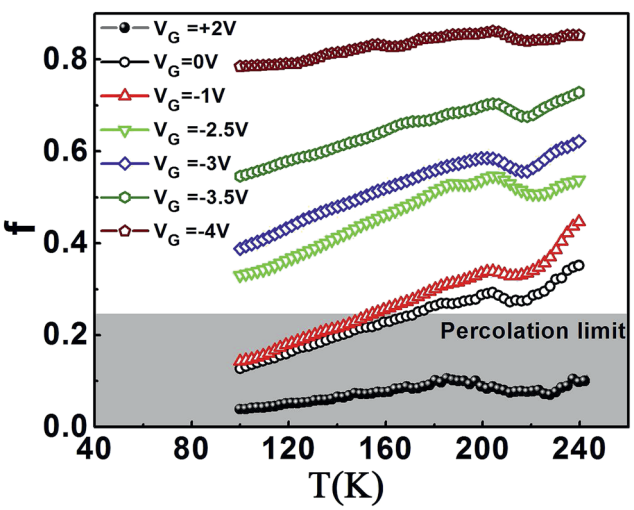

Fig. 8 Temperature dependence of f for different values of V_G.

the channel, in turn, leads to a larger $f(T,V_G) \rightarrow 1$, and the temperature dependence of $f(T,V_G)$ also becomes less steep due to the predominance of the metallic fraction. For $V_G \approx -3$ V and beyond, it is more or less T independent. For positive V_G ($\geq$2 V), the metallic fraction $f(T,V_G)$ is below the percolation limit for volume percolation[28] ($f_P = 0.25$), and the insulating phase makes a predominant contribution to the transport as $f(T,V_G)$ is $<f_P$. $f(T,V_G)$ depends on both T and the gate bias V_G. The explicit dependence of $f(T,V_G)$ on T is given by $f_0(T)$, which gives the temperature variation for zero bias. The scaled quantity $f(T,V_G)/f_0$ would thus show an explicit dependence of the fraction f on the applied gate bias. If we consider the scenario wherein the gate bias control of f predominantly occurs due to the control of the GB conductivity by V_G, then one would expect that $f(T,V_G)/f_0$ is directly proportional to the GB conductance G_{GB}. It has been established experimentally that the GB conductance is controlled primarily by tunneling at the GB.[16,29,30] The tunneling takes place through a depletion layer of thickness t, which is given by $t = \sqrt{\frac{2\varepsilon_0\varepsilon_r\phi_{GB}}{e^2 n_{3D}}}$, where ϕ_{GB} is the GB potential barrier. G_{GB} is $\propto$ to $\exp(-\chi t)$, where the inverse tunneling length $\chi = \sqrt{\frac{2m\phi_{GB}}{h^2}}$. Thus G_{GB} will be determined by the χt product, where $\chi t = \sqrt{\frac{4m\varepsilon_0\varepsilon_r}{e^2h^2n_{3D}}}\phi_{GB}$. The application of the gate bias will change both the barrier ϕ_{GB} and n_{3D} leading to a change in G_{GB} and thus $f(T,V_G)/f_0$. The GB barrier ϕ_{GB} has an inverse dependence on gate bias V_{GB}, as established through such studies on polycrystalline semiconductors.[31] Using the above discussion, we argue that $f(T,V_G)/f_0$ will have an exponential dependence on V_G and we can write the dependence of $f(T,V_G)$ on T and V_G as:

$$f = f_0(T)\exp\left(-\frac{V_G}{V_0}\right), \quad (2)$$

where $f_0(T)$ describes the T dependent evaluation of f at $V_G = 0$ as stated before. The scaling voltage V_0 may itself have a weak T dependence because it can have a dependence on ε_r as well as on n_{3D}, both of which have a T dependence (note: the T dependence of n_{3D} occurs due to dependence of λ_D on ε_r). To check the validity of the above relationship, we plot a scaled graph where $\ln f(T,V_G)/f_0$ is plotted *vs.* V_G/V_0. We find that all of the data for f can be merged onto a scaled curve that has a single parameter V_0. The values of V_0 at each T used to merge all of the data onto a single curve are shown in the inset. Fig. 9 establishes the exponential dependence of the fraction f on the gate bias and it shows that the phase control is predominantly brought about by the control of the potential barrier ϕ_{GB}. The parameter $V_0(T)$ has a linear dependence on T.

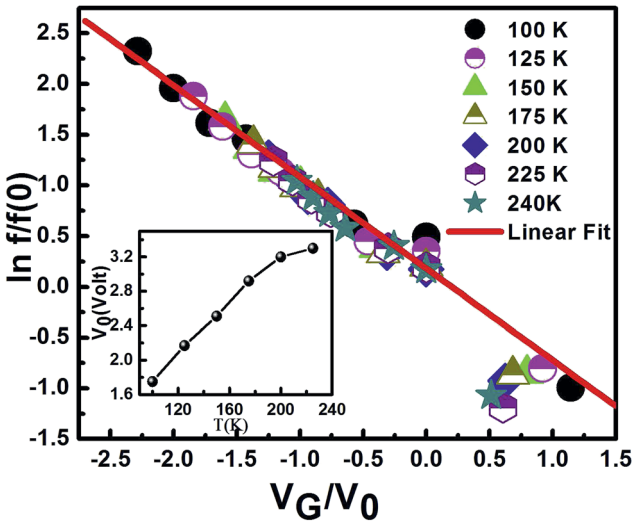

Fig. 9 Field dependence of the scaled $f(V,T)/f_0$ with respect to V_G/V_0. The inset shows the T dependence of $V_0(T)$.

8 Conclusions

In conclusion, we have shown that by using a gate dielectric with an EDL, it is possible to control the relative fraction of the coexisting phases in a film of low-hole doped $La_{1-x}Ca_xMnO_3$ with $x = 0.15$. The FE induced charge not only changes the resistance of the film (the channel in the FET device), it also changes the relative fraction f of the co-existing phases as well as the characteristic temperatures $T_{OO'}$, T_C^* and T_{FI}. The substantial control of the gate bias on the co-existing phases as well as on the charge transport in such films has been enabled by the effect of the gate bias on ϕ_{GB}, which in effect controls the GB transport. We have shown that the exponential control of the gate bias V_G on f originates from the predominant control of ϕ_{GB} by V_G. We have also shown that the change brought about by the FE closely mimics (quantitatively) that obtained *via* chemical substitution. One of the important observations in this study is that the FE can change the O–O′ transition temperature, which is a characteristic feature, identifiable from the resistance data. While $T_{OO'}$ is decreased upon hole accumulation, the ferromagnetic transition temperature T_C^* is increased. Though we could not establish the increase of T_C^* with an applied gate bias through direct magnetic measurements, it is intriguing that such a moderate gate bias (with an EDL dielectric) can lead to an appreciable hole density enhancement, such that the onset of the FM transition can be so much enhanced. This behavior compares very well to the phase-diagram of $La_{1-x}Ca_xMnO_3$ when x is changed by substitution.

Acknowledgements

The authors acknowledge the financial support from the Department of Science and Technology, Government of India as a sponsored project as a Unit for Nanoscience. R.N. acknowledges the support from CSIR as a Senior Research Fellowship. A.K.R. acknowledges J.C. Bose Fellowship for additional support.

References

1 K. Ueno, *et al.*, *Nat. Mater.*, 2008, **7**, 855–858.
2 Y. Lee, C. Clement, J. Hellerstedt, L. K. Joseph Kinney, X. Leng, S. D. Snyder and A. M. Goldman, *Phys. Rev. Lett.*, 2011, **106**, 136809.

3 M. Lee, J. R. Williams, S. Zhang, C. D. Frisbie and D. Goldhaber-Gordon, *Phys. Rev. Lett.*, 2011, **107**, 256601.
4 T. Hatano, Y. Ogimoto, N. Ogawa, M. Nakano, S. Ono, Y. Tomioka, K. Miyano, Y. Iwasa and Y. Tokura, *Sci. Rep.*, 2013, **3**, 2904.
5 A. T. A. O. M. K. Hongtao Yuan, H. Shimotani and Y. Iwasa, *Adv. Funct. Mater.*, 2009, **19**, 1046.
6 H. Yuan, H. Shimotani, J. Ye, S. Yoon, H. Aliah, A. Tsukazaki, M. Kawasaki and Y. Iwasa, *J. Am. Chem. Soc.*, 2010, **132**, 18403.
7 H. Du, X. Lin, Z. Xu and D. Chu, *J. Mater. Sci.*, 2015, **50**, 5641–5673.
8 K. Ueno, S. Nakamura, H. Shimotani, H. T. Yuan, N. Kimura, T. Nojima, H. Aoki, Y. Iwasa and M. Kawasaki, *Nat. Nanotechnol.*, 2011, **6**, 408.
9 A. S. Dhoot, C. Israel, X. Moya, N. D. Mathur and R. H. Friend, *Phys. Rev. Lett.*, 2009, **102**, 136402.
10 H. Shimotani, H. Asanuma, A. Tsukazaki, A. Ohtomo, M. Kawasaki and Y. Iwasa, *Appl. Phys. Lett.*, 2007, **91**, 082106.
11 R. Nath and A. K. Raychaudhuri, *Appl. Phys. Lett.*, 2014, **104**, 083515.
12 R. Mahesh, R. Mahendiran, A. K. Raychaudhuri and C. N. R. Rao, *Appl. Phys. Lett.*, 1996, **68**, 2291.
13 B. Ghosh, S. Kar, L. K. Brar and A. K. Raychaudhuri, *J. Appl. Phys.*, 2005, **98**, 094302.
14 M. A. Paranjape, K. S. Shankar and A. K. Raychaudhuri, *J. Phys. D: Appl. Phys.*, 2005, **38**, 3674.
15 T. Sarkar, M. V. Kamalakar and A. K. Raychaudhuri, *New J. Phys.*, 2012, **14**, 033026.
16 J. Klein, C. Hofener, S. Uhlenbruck, L. Alff, B. Buchner and R. Gross, *Europhys. Lett.*, 1999, **47**, 371.
17 P. Schiffer, A. P. Ramirez, W. Bao and S.-W. Cheong, *Phys. Rev. Lett.*, 1995, **75**, 3336.
18 R. Mahendiran, S. Tiwary, A. Raychaudhuri, T. Ramakrishnan, R. Mahesh, N. Rangavittal and C. Rao, *Phys. Rev. B: Condens. Matter Mater. Phys.*, 1996, **53**, 3348.
19 E. Dagotto, H. Takashi and A. Moreo, *Phys. Rep.*, 2001, **344**, 1–153.
20 H. Jain, A. Raychaudhuri, Y. M. Mukovskii and D. Shulyatev, *Solid State Commun.*, 2006, **138**, 318.
21 C. Ritter, M. R. Ibarra, J. M. D. Teresa, P. A. Algarabel, C. Marquina, J. Blasco, J. Garcia, S. Oseroff and S. W. Cheong, *Phys. Rev. B: Condens. Matter Mater. Phys.*, 1997, **56**, 8902.
22 Y. Zhou and S. Ramanathan, *Crit. Rev. Solid State Mater. Sci.*, 2013, **38**, 286.
23 C. H. Ahn, J. M. Triscone and J. Mannhart, *Nature*, 2003, **424**, 1015.
24 J. L. Cohn, M. Peterca and J. J. Neumeier, *Phys. Rev. B: Condens. Matter Mater. Phys.*, 2004, **70**, 214433.
25 R. Thiyagarajan, N. Manivannan, S. Arumugam, S. E. Muthu, N. R. Tamilselvan, C. Sekar, H. Yoshino, K. Murata, M. O. Apostu, R. Suryanarayanan and A. Revcolevschi, *J. Phys.: Condens. Matter*, 2012, **24**, 136002.
26 K. D. Chandrasekhar, A. K. Das, C. Mitra and A. Venimadhav, *J. Phys.: Condens. Matter*, 2012, **24**, 495901.
27 H. Rahmouni, M. Smari, B. Cherif, E. Dhahrib and K. Khirounia, *Dalton Trans.*, 2015, **44**, 10457.
28 Q. Xue, *Phys. B*, 2003, **325**, 195.
29 N. Khare, U. Moharil, A. Gupta, A. Raychaudhuri and R. P. SP Pai, *Appl. Phys. Lett.*, 2002, **81**, 325.
30 M. Paranjape, J. Mitra, A. Raychaudhuri, N. Todd, N. Mathur and M. Blamire, *Phys. Rev. B: Condens. Matter Mater. Phys.*, 2003, **68**, 144409.
31 T. Serikawa, S. A. Okamoto and S. Suyama, *IEEE Trans. Electron Devices*, 1984, **34**, 321.

